HHS Public Access

Author manuscript

Nature. Author manuscript; available in PMC 2018 December 31.

Published in final edited form as:

Nature. 2018 June ; 558(7711): 615–619. doi:10.1038/s41586-018-0239-3.

Epigenetic inheritance mediated by coupling of RNAi and histone H3K9 methylation

Ruby Yu, **Xiaoyi Wang**, and **Danesh Moazed**

Department of Cell Biology and Howard Hughes Medical Institute, Harvard Medical School, Boston MA 02115, USA.

Abstract

Histone posttranslational modifications (PTMs) are associated with epigenetic states that form the basis for cell type specific gene expression[1,2]. Once established, histone PTMs can be maintained by positive feedback involving enzymes that recognize and catalyze the same modification on newly deposited histones. Recent studies suggest that in wild-type cells, histone PTM-based positive feedback is too weak to mediate epigenetic inheritance in the absence of other inputs[3–7]. RNAi-mediated histone H3 lysine 9 methylation (H3K9me) and heterochromatin formation define a potential epigenetic inheritance mechanism in which positive feedback involving small interfering RNA (siRNA) amplification can be directly coupled to histone PTM positive feedback[8–14]. However, it remains unknown whether such a coupling of two feedback loops can maintain epigenetic silencing independently of DNA sequence and in the absence of enabling mutations that disrupt genome-wide chromatin structure or transcription[15–17]. Here using fission yeast *S. pombe*, we show that siRNA-induced H3K9me and silencing of a euchromatic gene can be epigenetically inherited in *cis* during multiple mitotic and meiotic cell divisions in wild-type cells. This inheritance involves the spreading of secondary siRNAs and H3K9me3 to the targeted gene and surrounding areas and requires both RNAi and H3K9me, suggesting that siRNA and H3K9me positive feedback loops act synergistically to maintain silencing. In contrast, when maintained solely by histone PTM positive feedback, silencing is erased by H3K9 demethylation promoted by Epe1, or by interallelic interactions following mating to cells containing an expressed epiallele even in the absence of Epe1. These findings demonstrate that the RNAi machinery can mediate transgenerational epigenetic inheritance independently of DNA sequence or enabling mutations and reveal a role for the coupling of siRNA and H3K9me positive feedback loops in protection of epigenetic alleles from erasure.

Correspondence: danesh@hms.harvard.edu. Reprints and permissions information is available at www.nature.com/reprints.

Author Contributions

R.Y. and D.M. conceived the project; R.Y. and X.W. performed experiments; R.Y. designed and performed experiments examining the endogenous *ade6*$^{+}$ locus and made the discovery of homologous erasure; X.Y. designed and performed experiments examining non-endogenous *ade6*$^{+}$ transgenes, comparing hairpin versus cen siRNA triggers, and deletion of *vtc4*$^{+}$/*rpl3402*$^{+}$, and repeated several experiments; R.Y. analyzed all the sequencing libraries; R.Y. and D.M. wrote the paper; all authors discussed results and participated in editing the manuscript.

The authors declare no competing financial interests.

Data availability. Genome-wide data sets are deposited at GEO under the accession number GSE111859.

To determine whether siRNA positive feedback loops participate in allele-specific inheritance of epigenetic states, we used a *cen::ade6*$^{+}$ transgene, which is epigenetically silenced and produces abundant *ade6*$^{+}$ siRNAs (Fig. 1a)[10,18]. Silencing of *ade6*$^{+}$ causes cells to grow red on medium with limiting adenine (Low Ade) (Fig. 1b, top), providing a visual assay for silencing. Previous studies have shown that the ability of siRNAs to mediate *de novo* silencing in *trans* is antagonized by mRNA 3'UTR processing pathways[16,17]. Consistently, we found that a second copy of *ade6*$^{+}$ located at its native euchromatic locus (hereafter referred to as 'endogenous *ade6*$^{+}$') remained refractory to silencing by siRNAs produced from the *cen::ade6*$^{+}$ transgene, as cells with both copies of *ade6*$^{+}$ always formed white colonies (Fig. 1b, middle). However, deletion of a subset of genes that influence mRNA transcription, 3' end processing, or export resulted in the appearance of red colonies at a frequency of 0.5–12%, indicating establishment of silencing at the endogenous *ade6*$^{+}$ allele (Fig. 1c, Extended Data Fig. 1a-c, white arrows). These included deletions of *mlo3*$^{+}$ and *dss1*$^{+}$, subunits of the conserved UAP56 mRNA export complex[19], histone acetyltranferase *mst2*$^{+}$, and *leo1*$^{+}$, a member of the Paf1 complex that negatively regulates RNAi-mediated silencing[17]. When isolated and re-plated, these red colonies produced mostly red colonies (~85%, Fig. 1c, Extended Data Fig 1b-c), indicating that the silent state was stably inherited. Silencing was accompanied by spreading of H3K9me at the endogenous *ade6*$^{+}$ locus into the adjacent *vtc4*$^{+}$ gene (Fig. 1d-e; Extended Data Fig. 1d-e). Furthermore, as expected for H3K9me3-mediated transcriptional gene silencing, we observed reduced RNA pol II occupancy at *vtc4*$^{+}$ that was specifically associated with *ade6*$^{+}$-OFF/red cells relative to non-silenced white control cells (Extended Data Fig. 1f-h).

To further investigate the mechanism of *ade6*$^{+}$ silencing, we determined whether trigger *cen::ade6*$^{+}$ siRNAs induced the generation of secondary siRNAs at endogenous *ade6*$^{+}$ by small RNA sequencing (sRNA-seq) in *cen::ade6*$^{+}$ *ade6*$^{+}$ *mlo3Δ* cells that expressed (ON/white) or silenced (OFF/red) *ade6*$^{+}$. As shown in Fig. 1f, we observed spreading of siRNAs outside the region of homology with *cen::ade6*$^{+}$ (denoted by the grey shaded area) for both the ON and OFF epigenetic states, but siRNAs only spread to adjacent *vtc4*$^{+}$ in *ade6*$^{+}$-OFF cells. We observed no siRNA spreading in *cen::ade6*$^{+}$ *ade6*$^{+}$ or *cen*$^{+}$ *ade6*$^{+}$ *mlo3Δ* cells, indicating that the biogenesis of secondary siRNAs required trigger centromeric *ade6*$^{+}$ siRNAs and *mlo3Δ* (Fig. 1f, top 2 tracks). siRNA spreading correlated with the spreading of H3K9me2 and H3K9me3 into *vtc4*$^{+}$ only in *ade6*$^{+}$-OFF cells (Fig. 1d-e). These results indicate that in *mlo3Δ* cells, siRNAs produced from a centromeric transgene can act in *trans* to silence a euchromatic copy of the gene, and that this silencing is accompanied by the generation of euchromatic secondary siRNA and H3K9me. Furthermore, even though silencing is established at a low frequency, it is maintained at a high frequency, suggesting that maintenance of silencing involves epigenetic memory.

To investigate whether epigenetic memory at the endogenous *ade6*$^{+}$ locus could be maintained in the absence of the *mlo3Δ* enabling mutation or *cen::ade6*$^{+}$ siRNAs, we introduced silent mutations into the endogenous *ade6*$^{+}$ allele (*ade6*$^{BC+}$, barcoded allele) so that it could be distinguished from *cen::ade6*$^{+}$ or *ade6*$^{+}$ by PCR (Fig. 2a). We crossed *cen::ade6*$^{+}$ *mlo3Δ* *ade6*$^{+}$-OFF/red to *cen*$^{+}$ *ade6*$^{BC+}$-ON/white cells and analyzed the haploid meiotic progeny. As shown in Fig. 2b-c and Extended Data Fig. 2a, the OFF state was stably transmitted to wild-type progeny, whether *cen::ade6*$^{+}$ was present or not. Furthermore, the

acquired silent state was remarkably stable, as nearly 50% of the *cen*$^{+}$ *ade6*$^{+}$ cells remained red after 32 generations (Fig. 2c, right). Importantly, analysis of the red and white progeny by allele-specific PCR showed that all OFF/red progeny of the cross contained the parental *ade6*$^{+}$-OFF allele, indicating that the silent state was transmitted in an allele-specific manner (Fig. 2b).

To determine the genetic requirements for maintenance of the silent allele, we performed the above cross with cells lacking key RNAi genes (*ago1Δ*, *dcr1Δ*, *rdp1Δ*) or the H3K9 methyltransferase (*clr4Δ*). The results indicated that silencing of endogenous *ade6*$^{+}$ required both the RNAi pathway and Clr4 (Fig. 2d-g and Extended Data Fig 2b-e, no red *ago1Δ*, *dcr1Δ*, *rdp1Δ* or *clr4Δ* progeny). Thus *cis* silencing of *ade6*$^{+}$ is maintained epigenetically by an RNAi- and H3K9 methylation-dependent mechanism, independently of the initial *cen::ade6*$^{+}$ siRNA trigger or any mutation that disrupts normal RNA processing.

Epigenetic inheritance of a *trp1*$^{+}$*::ade6*$^{+}$ transgene, induced by hairpin siRNAs targeting *ade6*$^{+}$, has been previously observed in the absence of the hairpin trigger, but remained strictly dependent on enabling mutations in *leo1*$^{+}$ or other Paf1 subunits[17]. In contrast, here we observed epigenetic inheritance of *ade6*$^{+}$ silencing in the absence of both an enabling mutation and trigger siRNAs (Fig. 2). To investigate whether differences in the siRNA trigger or the enabling mutation account for the difference in heritability, we compared maintenance of silencing at the endogenous *ade6*$^{+}$ locus using either *cen::ade6*$^{+}$ or hairpin *ade6*$^{+}$ trigger siRNAs in *leo1Δ* cells. As shown in Extended Data Fig. 3a, both siRNA triggers induced endogenous *ade6*$^{+}$ silencing. We crossed cells with the above silent *ade6*$^{+}$ alleles to cells lacking both the siRNA trigger and the enabling *leo1Δ* mutation and examined silencing in the meiotic progeny. In contrast to *cen::ade6*$^{+}$-triggered silencing, hairpin-triggered *ade6*$^{+}$ silencing was lost in the *leo1*$^{+}$ segregants (Extended Data Fig. 3b-c). Furthermore, unlike *cen::ade6*$^{+}$, which induced a broad domain of secondary siRNAs, the hairpin triggered very low levels of secondary siRNAs that were restricted to the *ade6*$^{+}$ coding region (Extended Data Fig. 3d). ChIP-seq and ChIP-qPCR experiments showed that unlike the *cen::ade6*$^{+}$ trigger, which induced broad domains of H3K9 methylation at the *ade6*$^{+}$ locus, the hairpin trigger induced more restricted domains (Extended Data Fig. 3e-h). In particular, H3K9me3 levels were very low when silencing was induced by the hairpin and did not extend significantly beyond *ade6*$^{+}$ (Extended Data Fig. 3f, h). In this regard, we recently demonstrated that H3K9me3 is required for transcriptional gene silencing and epigenetic inheritance, while H3K9me2 is sufficient for RNAi-mediated co-transcriptional gene silencing[20]. We therefore conclude that the nature of the siRNA trigger, but not the enabling mutation, plays a critical role in spreading of secondary siRNAs and H3K9me that determines heritability of the epiallele.

Epigenetic states in yeast and animal cells can be transmitted in *cis* during cell division[21,22]. To address whether the siRNA positive feedback loop, which generates high levels of siRNA that can potentially act globally, could discriminate between identical target sequences to mediate *cis* (allele-specific) inheritance of epigenetic states, we took advantage of the *ade6*$^{BC+}$ allele, which is genetically identical to *ade6*$^{+}$ except for a few silent nucleotide substitutions (Figure 2a). We crossed wild-type cells carrying the siRNA-dependent *ade6*$^{+}$-OFF allele to wild-type cells carrying the *ade6*$^{BC+}$-ON allele (Fig. 2d-g, Fig. 3a), analyzing

the meiotic progeny to determine whether silencing was inherited in an allele-specific manner. As shown in Fig. 3a, the OFF/red and ON/white expression states segregated with a 2:2 Mendelian ratio. Moreover, allele-specific PCR showed that the OFF/red progeny contained the parental *ade6*$^{+}$-OFF allele and the ON/white progeny contained the parental *ade6*$^{BC+}$-ON allele, indicating that each state was stably and independently transmitted following meiosis. To rule out any role for the *ade6*$^{BC+}$ nucleotide substitutions, we performed the reciprocal cross and observed the same 2:2 segregation phenotype with faithful maintenance of the parental OFF allele (Extended Data Fig. 4a). In agreement with the tetrad dissection data, random spore analysis showed that 97.5% of OFF/red progeny contained the parental OFF allele (Fig. 3b). These results therefore demonstrate that an acquired silent state can be preferentially propagated in *cis* as an epiallele by an siRNA-dependent mechanism. The acquired silent state was furthermore stable through multiple meiotic cell divisions (Fig. 3c, Extended Data Fig 4b). This, together with the continuous dependence of silencing on RNAi (Fig. 2d-f), suggests that maintenance of silencing and heterochromatin relies on a continuous RNAi-dependent amplification mechanism.

We next investigated how siRNAs and H3K9me work together to maintain silencing at the *ade6*$^{+}$ epiallele. ChIP-seq analysis showed that silencing correlated with high levels of H3K9me2 and H3K9me3 at *ade6*$^{+}$ and the immediately downstream *vtc4*$^{+}$ and *rpl3402*$^{+}$ genes (Fig. 3d, Extended Data Fig. 5a, compare OFF and ON tracks for *cen*$^{+}$ cells). As controls, centromeric levels of H3K9me2 and H3K9me3 were comparable between samples (Extended Data Fig. 5b-c). Thus, consistent with the requirement for the Clr4 H3K9 methyltransferase, the silent *ade6*$^{+}$ epiallele was associated with high levels of H3K9me2 and H3K9me3. Sequencing of siRNAs showed that silencing in *ade6*$^{+}$-OFF cells correlated with accumulation of *vtc4*$^{+}$ and *rpl3402*$^{+}$ siRNAs (Fig. 3e, rows 4–7). In cells containing *cen::ade6*$^{+}$, we also observed secondary siRNA accumulation upstream of *ade6*$^{+}$, to tandem gene *bub1*$^{+}$, and about 10kb downstream of *ade6*$^{+}$ (Fig. 3e, rows 4–5), which correlated with increased spreading of H3K9me3 (Fig. 3d-e, colored asterisks highlight regions where H3K9me3 and siRNA reads correlate). Surprisingly, in cells lacking *cen::ade6*$^{+}$, we observed very few siRNA reads that mapped to *ade6*$^{+}$-OFF (Fig. 3e, rows 6–7 and Extended Data Fig. 5d, rows 6–7), and the vast majority of siRNA detected were produced from the adjacent *vtc4*$^{+}$ and *rpl3402*$^{+}$ genes. We therefore tested whether *vtc4*$^{+}$ and *rpl3402*$^{+}$ were required for maintenance of the *ade6*$^{+}$-OFF state, and found that *ade6*$^{+}$ silencing in *vtc4-rpl3402Δ* cells was only maintained in cells carrying the *leo1Δ* enabling mutation (Extended Data Fig. 6). These results indicate that an siRNA positive feedback loop, which forms at the adjacent *vtc4*$^{+}$ and *rpl3402*$^{+}$ genes, is required for epigenetic inheritance of the silent *ade6*$^{+}$ epiallele in wild-type cells. Consistent with a requirement for *vtc4*$^{+}$ in epigenetic inheritance of *ade6*$^{+}$ silencing, secondary siRNAs and H3K9me3 associated with non-heritable hairpin-induced silencing did not spread to the *vtc4*$^{+}$ gene (Extended Data Fig. 3). Together with the observation that the silencing activity of siRNAs is restricted to the epiallele that already possesses H3K9me (Fig. 3a, b), these results suggest that the mutual dependence of H3K9me and siRNA generation on each other underlies the mechanism of *cis* epigenetic inheritance.

To test possible effects of genomic context on siRNA-triggered silencing and its epigenetic inheritance, we inserted the *ade6*$^{+}$ gene together with a selectable marker (*KanR-ade6*$^{+}$) at

different euchromatic loci in cells containing the *cen::ade6*$^{+}$ siRNA trigger and an enabling mutation. We observed silencing at 4 transgene insertions (*mal1*$^{+}$*::KanR-ade6*$^{+}$, *efm3*$^{+}$*::KanR-ade6*$^{+}$, *meu10*$^{+}$*::KanR-ade6*$^{+}$, and *mrp1*$^{+}$*::KanR-ade6*$^{+}$), indicated by growth of red colonies on low adenine medium (Extended Data Fig. 7a-d). Furthermore, after diploid formation and sporulation, we observed epigenetic maintenance of the OFF state at each locus in meiotic progeny lacking both the siRNA trigger and the enabling mutation (extended Data Fig. 7e-h). The resulting OFF epialleles were stably maintained upon further mitotic propagation (Extended Data Fig. 7i), were associated with H3K9me3 (Extended Data Fig. 7j), and required Ago1 and Clr4 for epigenetic inheritance (*efm3*$^{+}$*::KanR-ade6*$^{+}$ and *meu10*$^{+}$*::KanR-ade6*$^{+}$ OFF/red epialleles) (Extended Data Fig. 7k-l). Furthermore, like the euchromatic endogenous *ade6*$^{+}$ locus (Fig. 1f), secondary siRNA generation extended to surrounding transcription units specifically in the OFF state (Extended Data Fig. 8). Therefore, the ability of siRNA-coupled H3K9me to mediate epigenetic inheritance is not restricted to a particular locus.

We previously demonstrated that artificial tethering of TetR-Clr4 upstream of an *ade6*$^{+}$ gene inserted at the *ura4*$^{+}$ locus (*ura4Δ::10XtetO-ade6*$^{+}$) results in H3K9me and silencing[3]. This RNAi-independent silencing can be inherited epigenetically after deletion of the TetR-Clr4 initiator, but only when H3K9 demethylation is decreased by deletion of *epe1*$^{+}$, which encodes a JmjC domain demethylase family member[3,23]. We therefore investigated whether deletion of *epe1*$^{+}$ could suppress the requirement for RNAi machinery in epigenetic maintenance of the *ade6*$^{+}$-OFF state. Crossing *cen::ade6*$^{+}$ *mlo3Δ ade6*$^{+}$-OFF cells to *cen*$^{+}$ *ago1Δ epe1Δ ade6*$^{+}$-ON cells produced 46 *ago1Δ epe1Δ* haploid progeny, 2 of which formed pink or red colonies (Fig. 4a, Extended Data Fig. 9a). Upon re-plating, these red colonies formed a mixture of red and white colonies, indicating that deletion of *epe1*$^{+}$ partially suppressed the requirement for RNAi in maintenance of the silent *ade6*$^{+}$ epiallele (Fig. 4a, right side). In contrast, all *ago1Δ epe1*$^{+}$ progeny lost *ade6*$^{+}$ silencing, demonstrating that RNAi counteracts Epe1-mediated erasure of the silent *ade6*$^{+}$ epiallele.

We next investigated whether the RNAi-independent OFF state of the *ura4Δ::10XtetO-ade6*$^{+}$ epiallele could be transmitted in *cis* in cells lacking the TetR-Clr4-I initiator[3], as is the case with the RNAi-dependent *ade6*$^{+}$-OFF allele (Fig. 3a). Consistent with previous findings[3], crossing an *epe1Δ ura4Δ::10XtetO-ade6*$^{+}$-OFF/red allele to another OFF/red allele produced haploid progeny that retained the OFF/red state at a high frequency (48%, Fig. 4b). However, when we crossed an *epe1Δ ura4Δ::10XtetO-ade6*$^{+}$-OFF/red allele to a genetically identical *epe1Δ ura4Δ::10XtetO-ade6*$^{+}$-ON/white allele, the resulting haploid progeny were mostly white, indicating that they had lost the silent state (0.01% *ade6*$^{+}$-OFF/red, Fig. 4c, d). Since the OFF x OFF *ura4Δ::10XtetO-ade6*$^{+}$ cross produces many (48%) *ade6*$^{+}$-OFF/red progeny, the epigenetic erasure event in the OFF x ON cross is not caused by a general change in chromatin structure during meiosis and is likely due to the proximity of the OFF and ON alleles during homolog pairing prior to or during meiosis. Consistent with this hypothesis, *ura4Δ::10XtetO-ade6*$^{+}$ silencing was maintained, although at a lower frequency than in an OFF x OFF cross, in a cross in which we disrupted homolog pairing by replacing *10XtetO-ade6*$^{+}$ with the non-homologous *ura4*$^{+}$ gene (Extended Data Fig. 9b-d). To determine whether siRNAs could protect a silent epiallele from homolog-induced erasure, as suggested in OFF x ON crosses involving the RNAi-dependent endogenous *ade6*$^{+}$ locus

(Fig. 2 and 3), we induced silencing at the *ura4Δ::ade6*$^{+}$ locus using *cen::ade6*$^{+}$ siRNAs instead of TetR-Clr4-I (Extended Data Fig. 10). In contrast to the RNAi-independent TetR-Clr4-I induced *ura4Δ::10X-tetO-ade6*$^{+}$ silent epiallele, which was erased in the progeny of the OFF x ON cross (Fig. 4d), the siRNA-induced *ura4Δ::ade6*$^{+}$ silent epiallele was maintained in nearly 40% of the meiotic progeny of the OFF x ON cross (Fig. 4e). Therefore, in addition to protection against Epe1-dependent erasure (Fig. 4a), siRNAs protect a silent epiallele against erasure by an expressed epiallele during homolog pairing.

In summary, our findings reveal that coupling of RNAi and H3K9me can mediate epigenetic inheritance of gene silencing. The role of siRNAs in allele-specific *cis* maintenance of an epigenetic state in *S. pombe* can be explained by the dual requirement for both siRNAs and histone H3K9me in recruitment of the RNAi-induced transcriptional silencing (RITS) complex, which in turn recruits Clr4 (Fig. 4f). Recently, a role for site-specific DNA binding proteins in epigenetic maintenance of silent chromatin was also described[5–7]. In contrast to site-specific DNA binding proteins, the siRNA-dependent epigenetic inheritance mechanism described here acts in a less sequence-dependent manner and can potentially transmit epigenetic silencing at any locus that allows autonomous siRNA amplification. Furthermore, the coupling of siRNA- and H3K9me-dependent recruitment protects the epigenetic state from erasure mechanisms, which may involve either removal of H3K9me by demethylases such as Epe1 or signals from an expressed allele during the pairing of homologous chromosomes. The latter is reminiscent of transvection in *Drosophila*, in which homolog pairing in diploid somatic cells allows positive regulatory elements on one homolog to activate gene expression on the other[24,25]. Based on their general requirement for epigenetic inheritance in *S. pombe*, we propose that specificity factors such as DNA-binding proteins and small or large noncoding RNAs act as important components of most epigenetic inheritance mechanisms.

Methods

Strain Constructions.

S. pombe strains used in this study are described in SI Table 1.

ChIP-qPCR.

ChIP experiments were performed as previously described[16], using anti-H3K9me2 (Abcam, ab1220), anti-H3K9me3 (Diagenode, C15500003), and anti-RNA Polymerase II (Covance, 8WG16) antibodies.

Sample preparation for multiplex ChIP-seq.

Libraries for Illumina sequencing were constructed following the manufacturer's protocols, starting with ~5 ng of immune-precipitated DNA fragments. Each library was generated with custom-made adapters carrying unique barcode sequence at the ligating end[26]. Barcoded libraries were mixed and sequenced with Illumina HiSeq2000. Raw reads were separated according to their barcodes and mapped to the *S. pombe* genome using Bowtie. Mapped reads were normalized to reads per million and visualized in IGV.

sRNA-seq.

To purify total sRNAs, cells were grown in 20 ml YES[27] to a concentration of ~2×10^7 cells/ml. Pellets were processed using the mirVana™ miRNA Isolation kit (Ambion), and the resulting RNA used for library construction. Total small RNA libraries were constructed as previously described[28]. Briefly, 21–30nt RNA was size-selected on a 17.5% polyacrylamide/7M urea gel and ligated to a 3' adapter. The ligated species were size-selected on a 17.5% polyacrylamide/7M urea gel and ligated to a 5' adapter. RNA was then reverse transcribed into cDNA and PCR-amplified in a two-step process. Amplified cDNA was gel-purified and sequenced on an Illumina High-Seq platform. Reads with maximum 1 nt mismatch were aligned to the *S. pombe* genome using Novoalign (http://www.novocraft.com/products/novoalign/), normalized for reads per million using a Python script, and visualized using IGV (http://www.broad.mit.edu/igv/). Reads mapping to more than one location were randomly assigned.

Code availability.

The Python script for converting Novoalign output to IGV-viewable files is included in Supplementary Information.

Quantitative PCR.

DNA or cDNA was amplified with the Taq polymerase using primers described in SI Table 2 in the presence of SYBR Green. For ChIP-qPCR, reported values are % of input using the ΔC_T method. Error bars in all figures indicate mean +/− standard deviation.

Spotting *ade6*$^+$ silencing assays.

Cells were either grown in 2 ml of rich medium (YEA, yeast extract plus adenine) at 30°C or picked from fresh plates. Cells were washed with water, then resuspended in water to a concentration of 2×10^4 or 2×10^5 cells/ml. 5 ul serial dilutions (between 5-fold and 2-fold) were then spotted on YE medium containing low adenine (Low Ade) for 3 to 5 days and photographed.

Random spore analysis and tetrad dissection.

Fresh colonies of each parental strain were mixed in 50 µl water, plated on low-nitrogen medium (ME), and incubated at 30°C for 2–3 days. For random spore analysis, one loopful of crossed cells was resuspended in 1 ml water and checked under a microscope for the presence of tetrads. The cell suspension was then incubated at room temperature overnight with 5 µl glusalase (Perkin Elmer) to kill non-spore cells, then diluted such that ~100–200 cells were spread onto each plate of yeast extract Low Ade medium. For tetrad dissection, cells were struck onto a Low Ade plate, and tetrads were separated using a Singer Instrument MSM System 400. Tetrads were incubated at 32°C for 3–6 hours, and individual spores were separated on the plate. Plates were then incubated at 32°C for 4–5 days and photographed.

Extended Data

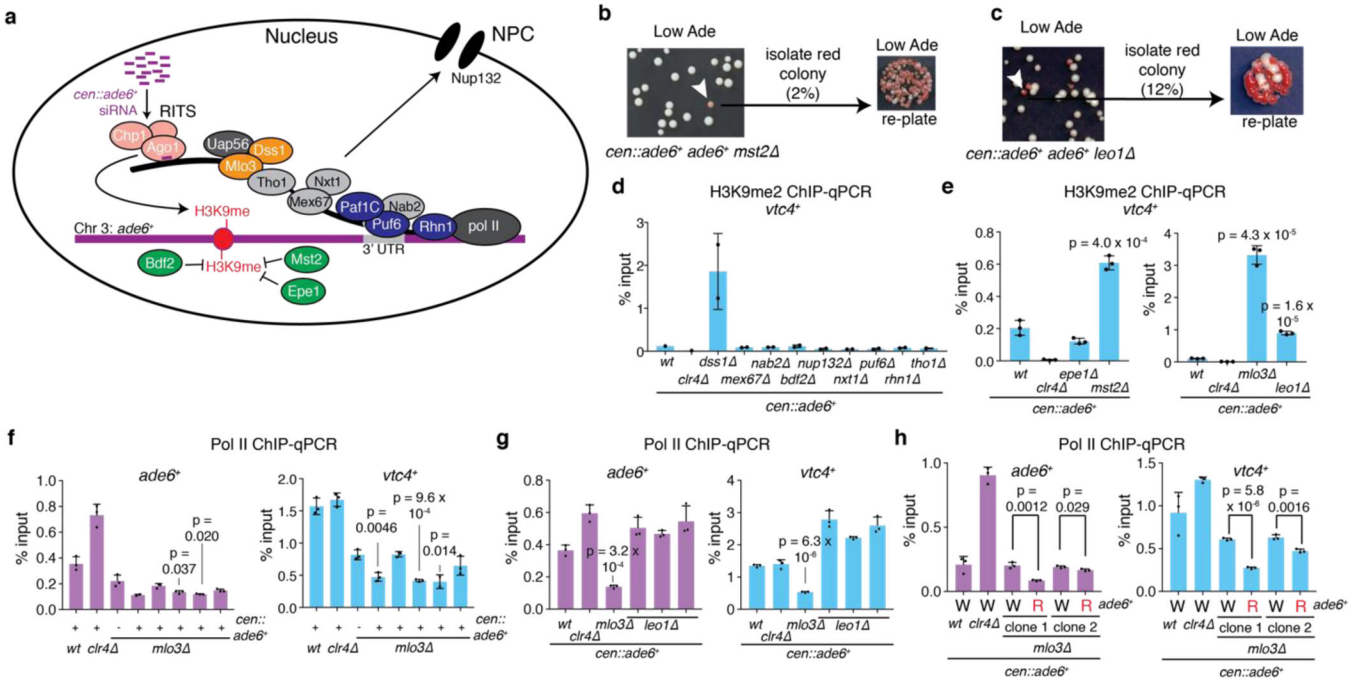

Extended Data Figure 1 |. siRNA-induced H3K9me3 at the euchromatic *ade6*$^+$ locus and flanking region.

a, Summary of pathways and factors involved in mRNA 3'end processing and its coupling to nuclear export. Chp1 and Ago1 are subunits of the RNAi-induced transcriptional silencing complex (RITS). Uap56 and Mlo3 are TREX (transcription-export) complex subunits, and associate with Dss1 to mediate mRNA export. Tho1 is a subunit of the THO/TREX complex, which is responsible for recruiting other subunits of the TREX complex to mRNA. Mex67 is an ortholog of human NXF1, a critical mRNA export receptor, and associates with Nxt1, another mRNA export factor. Puf6 is an mRNA 3'-UTR-binding protein that has been shown to associate with Mlo3. Rhn1 is involved in RNA Pol II transcriptional termination. Nab2 is a poly(A)-binding protein. The Paf1 complex is required for transcriptional elongation and 3' end processing, and mutations in Paf1 subunits allow siRNA-mediated heterochromatin formation and silencing of euchromatic genes. Nup132 is a component of the nuclear pore complex (NPC) that has been linked to mRNA export factors. Bdf2 is a histone binding protein that has been shown to inhibit the spreading of centromeric heterochromatin. Epe1 is a jmjC-domain containing putative demethylase that also promotes spreading of heterochromatin. Mst2 is a histone aceyltransferase. See main text for references.

b-c, Around 1000 *cen::ade6*$^+$ *mst2*Δ (**b**) or *cen::ade6*$^+$ *leo1*Δ (**c**) cells were plated on low adenine medium (Low Ade). Most cells formed white colonies, indicating expression of endogenous *ade6*$^+$, while ~2% of *mst2*Δ (**b**) and 12% of *leo1Δ* (**c**) cells formed red or pink colonies, indicating silencing of endogenous *ade6*$^+$ (white arrow). Upon replating, the resulting red colonies formed mostly red colonies, indicating efficient maintenance of the silent state. Repeated once with similar results for each.

d-e, ChIP-qPCR assays showing mean +/− SD H3K9me2 levels at the *vtc4*$^{+}$ locus, which is located next to the *ade6*$^{+}$ gene, in the indicated mutant cells based on 2 (**d**) or 3 (**e**) independent clones. p values are based on a 2-tailed Student's t-test comparing the indicated mutants to wild-type cells.

f-h, ChIP-qPCR assays showing mean +/− SD Pol II occupancy at the *ade6*$^{+}$ (purple) or *vtc4*$^{+}$ (blue) locus in *mlo3Δ* or *leo1Δ* clones that have not been selected for silencing (99.5% and 88% white, respectively); p values are based on a 2-tailed Student's t-test comparing the indicated mutants to wildtype cells (**f-g**). In (**h**), either an *ade6*$^{+}$-ON (W) or *ade6*$^{+}$-OFF (R) colony from each of two clones was picked for analysis. p values based on a 2-tailed Student's t-test comparing the indicated red to white cells for each clone. 3 biological replicates were used per sample.

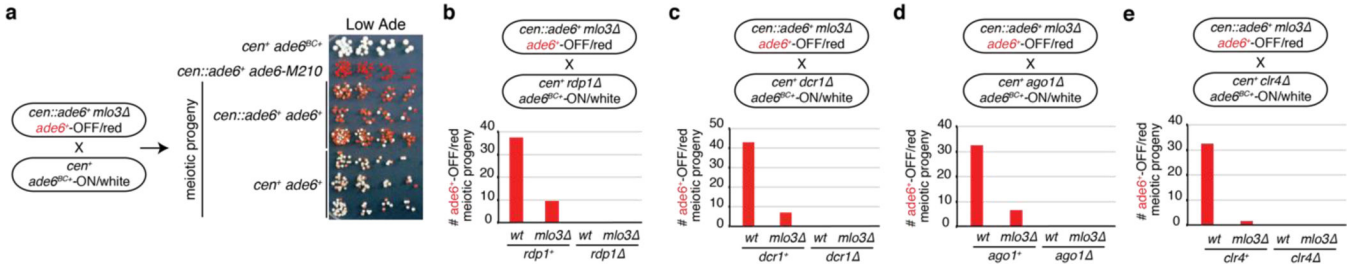

Extended Data Figure 2 |. The acquired *ade6*$^{+}$ silent allele is stable in the absence of the *cen::ade6*$^{+}$ siRNA trigger and the *mlo3Δ* enabling mutation.

a, *ade6*$^{+}$-OFF *progeny* of the cross in Fig. 2b with the indicated genotypes were plated on Low Ade medium. See Fig 2c for related results.

b-e, Biological replicates of the crosses shown in Fig. 2d-g. *cen::ade6*$^{+}$ *mlo3Δ ade6*$^{+}$-OFF cells were crossed to *cen*$^{+}$ *mlo3*$^{+}$ *ade6*$^{BC+}$-ON cells with deletions of key RNAi components **(b-d)** or H3K9 methyltransferase Clr4 (**e**) followed by RSA. All *ade6*$^{+}$-OFF progeny were *RNAi*$^{+}$ and *clr4*$^{+}$. Bars indicate number of *ade6*$^{+}$-OFF meiotic progeny for each genotype.

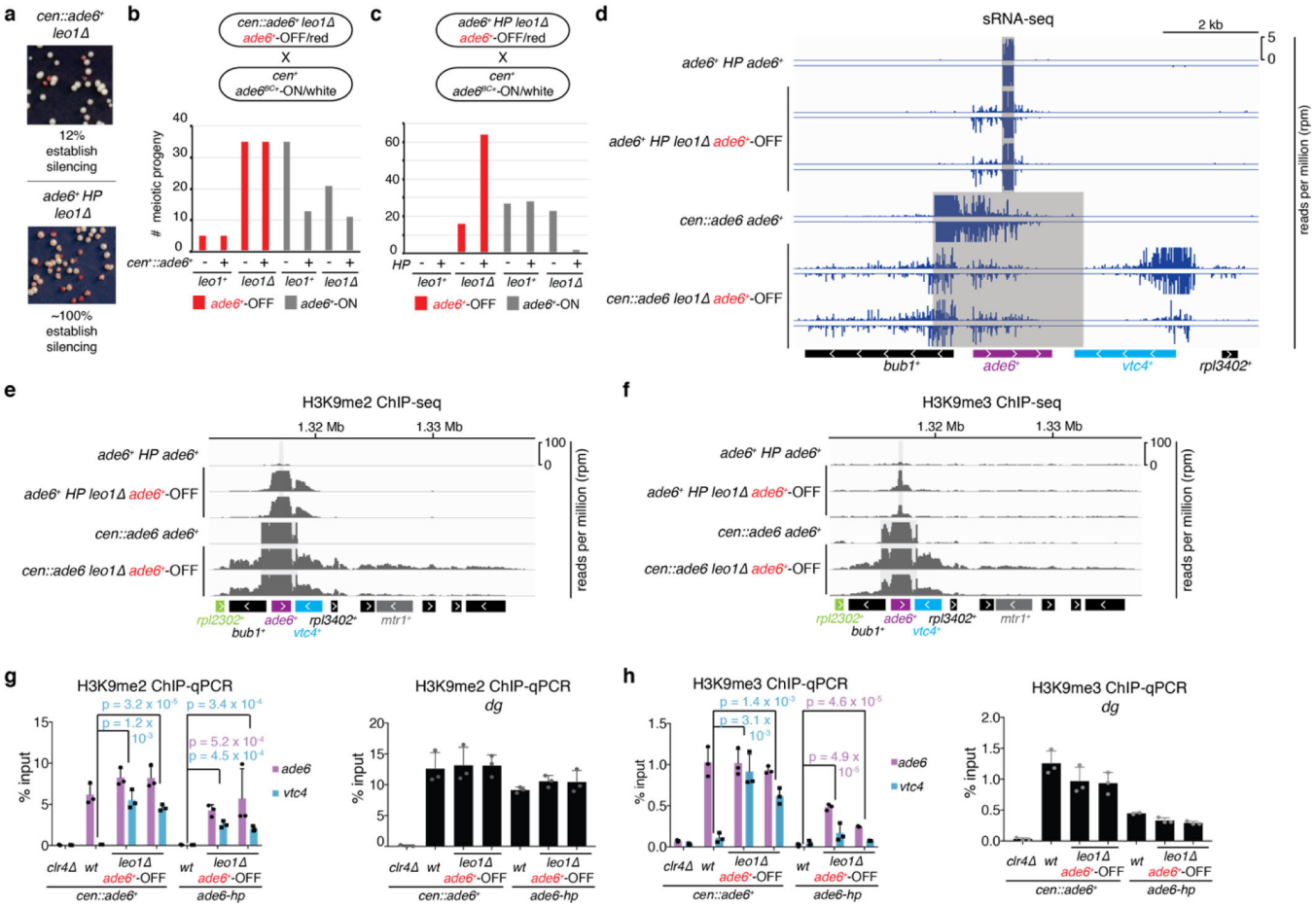

Extended Data Figure 3 |. The siRNA driver locus is critical for establishing a heritable silent epiallele

a, *cen::ade6*$^{+}$ *leo1*Δ (left) or *ade6*$^{+}$ hairpin (*HP) leo1*Δ (right) cells were plated on low adenine medium. ~12% of *cen::ade6*$^{+}$ *leo1*Δ (left) and 100% of *ade6*$^{+}$ *HP leo1*Δ (right) cells formed red or pink colonies, indicating silencing of endogenous *ade6*$^{+}$. Repeated twice.

b-c, *cen::ade6*$^{+}$ *ade6*$^{+}$-OFF *leo1Δ* cells (**b**) or *ade6*$^{+}$ *HP ade6*$^{+}$-OFF *leo1Δ* (**c**) cells were crossed to *cen*$^{+}$ *ade6*$^{BC+}$-ON cells followed by random spore analysis (RSA). Number of progeny matching each indicated genotype and phenotype is shown. 80 red and 80 white colonies were genotyped by PCR. Results reflect two independent crosses.

d, siRNA-sequencing showing limited secondary siRNA generation in *ade6*$^{+}$ *HP leo1Δ ade6*$^{+}$-OFF cells, compared with more extensive secondary siRNA spreading to neighboring genes *bub1*$^{+}$ and *vtc4*$^{+}$ in *cen::ade6*$^{+}$ *leo1Δ ade6*$^{+}$-OFF cells. Shaded areas represent sequence identity to *ade6*$^{+}$ *HP* (top 3 rows) or *cen::ade6*$^{+}$ (bottom 3 rows). Two independent clones shown for each experimental sample.

e-f, H3K9me2 (**e**) and H3K9me3 (**f**) ChIP-seq reads mapping to the endogenous *ade6*$^{+}$ locus in cells with the indicated genotypes and expression states. Shaded areas represent sequence identity to *ade6*$^{+}$ *HP* (top 3 rows) or *cen::ade6*$^{+}$ (bottom 3 rows). Two independent clones shown for each experimental sample.

g-h, ChIP-qPCR assays showing differences in H3K9me2 (**g**) or H3K9me3 (**h**) levels in *cen::ade6*$^{+}$ *leo1Δ ade6*$^{+}$-OFF and *ade6*$^{+}$ *HP leo1Δ ade6*$^{+}$-OFF cells at *ade6*$^{+}$ (purple) and

vtc4^{+} (blue). Bars reflect mean +/− SD from 3 biological replicates. p values are based on 2-tailed Student's t-test comparing *leo1Δ* cells to appropriate wild-type cells. On the right, control ChIP-qPCR at *dg* repeats.

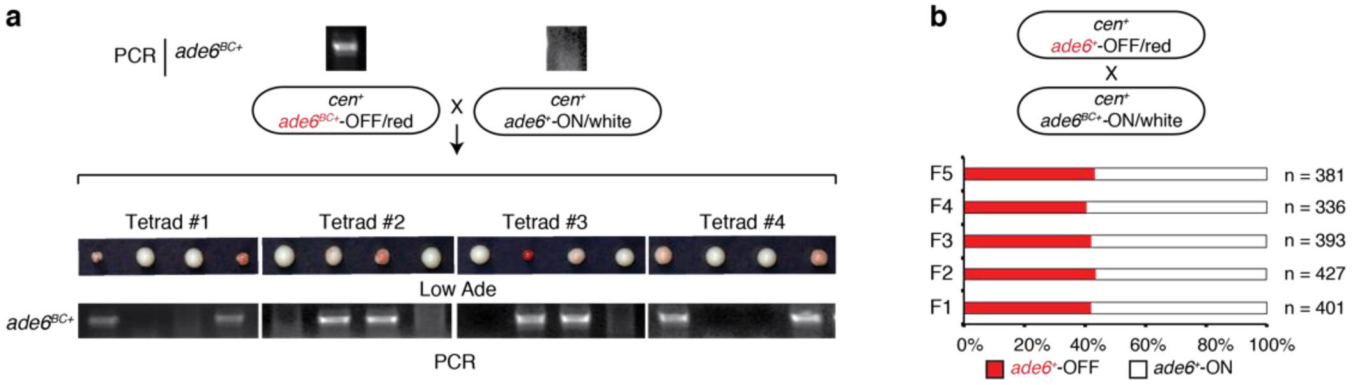

Extended Data Figure 4 |. cis inheritance of the acquired *ade6*$^{+}$ silencing and its stable propagation over multiple meiotic generations.

a, *ade6*^{BC}-OFF cells crossed to *ade6*$^{+}$-ON cells, followed by tetrad dissection on Low Ade medium (top) and genotyping using allele-specific PCRs (bottom), showed the 2:2 segregation of the OFF and ON states and *cis* transmission of each state. Performed once, but see Fig. 3a for reciprocal cross. **b,** *ade6*$^{+}$-OFF progeny of repeated *ade6*$^{+}$-OFF x *ade6*$^{BC+}$-ON crosses were selected and crossed again, showing stability of the *ade6*$^{+}$-OFF allele over five meiotic generations. n, number of meiotic progeny analyzed. Independent replicate of cross in Fig. 3c.

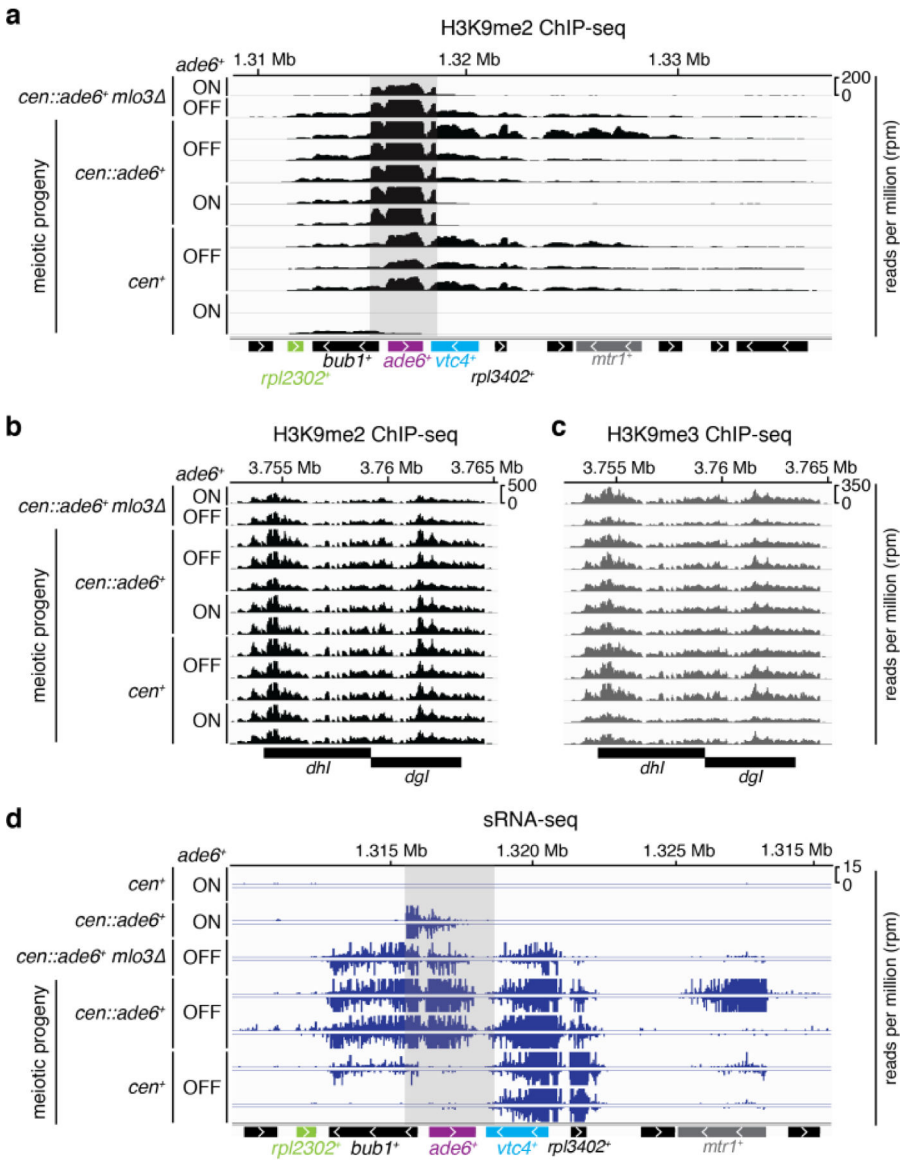

Extended Data Figure 5 |. Induction of H3K9me and siRNAs at the endogenous *ade6*$^+$ locus.
a, H3K9me2 ChIP-seq reads mapping to the endogenous *ade6*$^+$ locus in cells with the indicated genotypes and expression states. Shaded area indicates the region of sequence identify with *cen::ade6*$^+$. **b-c,** H3K9me2 (**b**) and H3K9me3 (**c**) ChIP-seq reads mapping to the *dg* and *dh* repeats of centromere 1 (*dg1* and *dh1*, respectively) in cells with the indicated genotypes and phenotypes. **d,** Zoomed in view of sRNA-seq reads at the endogenous *ade6*$^+$ locus shown in Fig. 3e. Shaded area indicates *cen::ade6*$^+$ homology. 2–3 independent clones were sequenced each for ON and OFF meiotic progeny.

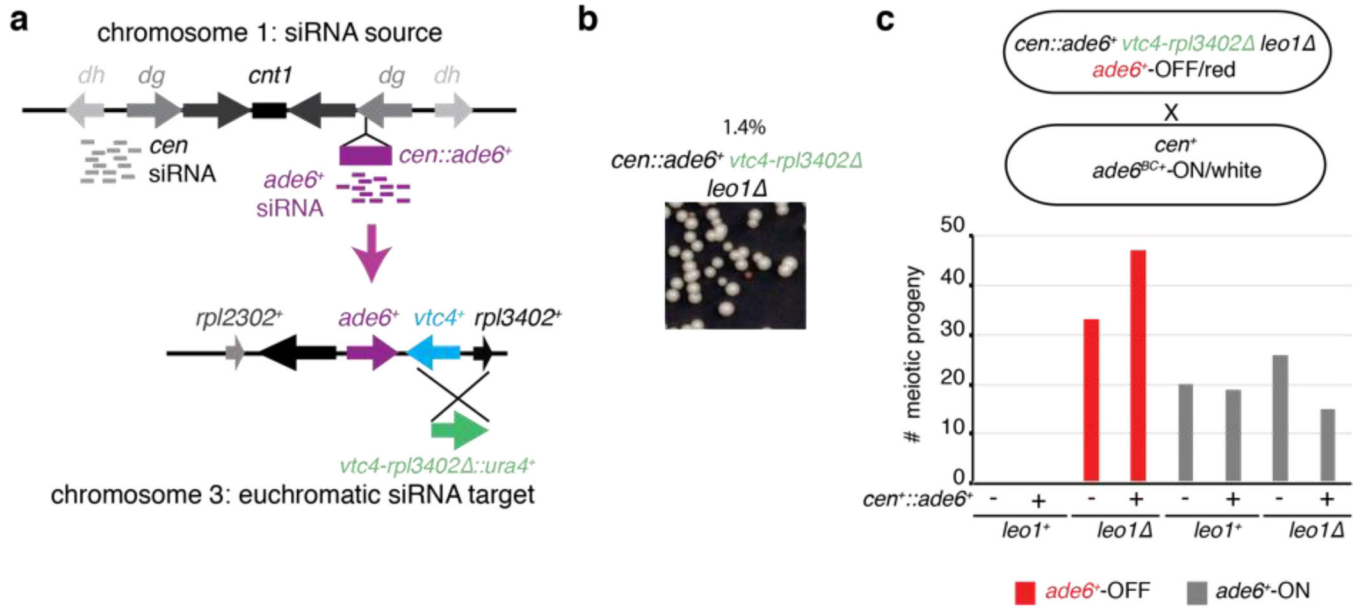

Extended Data Figure 6 |. *vtc4*$^{+}$ and *rpl3402*$^{+}$ are critical for inheritance of silencing at the endogenous *ade6*$^{+}$ locus.

a, Schematic of the siRNA driver *cen::ade6*$^{+}$ locus on chromosome 1 (upper) and the endogenous *ade6*$^{+}$ locus (lower) in which the *vt4*$^{+}$ and *rpl3402*$^{+}$ genes were replaced with the *ura4*$^{+}$ gene (*vtc4-rpl3402Δ::ura4*$^{+}$). **b,** Frequency of silencing establishment at endogenous *ade6*$^{+}$ in *cen::ade6*$^{+}$ *leo1Δ vtc4-rpl3402Δ* cells. Repeated twice. **c,** *cen::ade6*$^{+}$ *leo1Δ vtc4-rpl3402Δ ade6*$^{+}$-OFF cells were crossed to *cen*$^{+}$ *leo1*$^{+}$ *ade6*$^{BC+}$-ON cells followed by random spore analysis (RSA) to test the epigenetic maintenance of the OFF state in the absence of the *cen::ade6*$^{+}$ siRNA driver and the *leo1Δ* enabling mutation. The number of progeny matching each genotype and phenotype are shown. 80 white and 80 red progeny were genotyped. Results reflect two independent crosses.

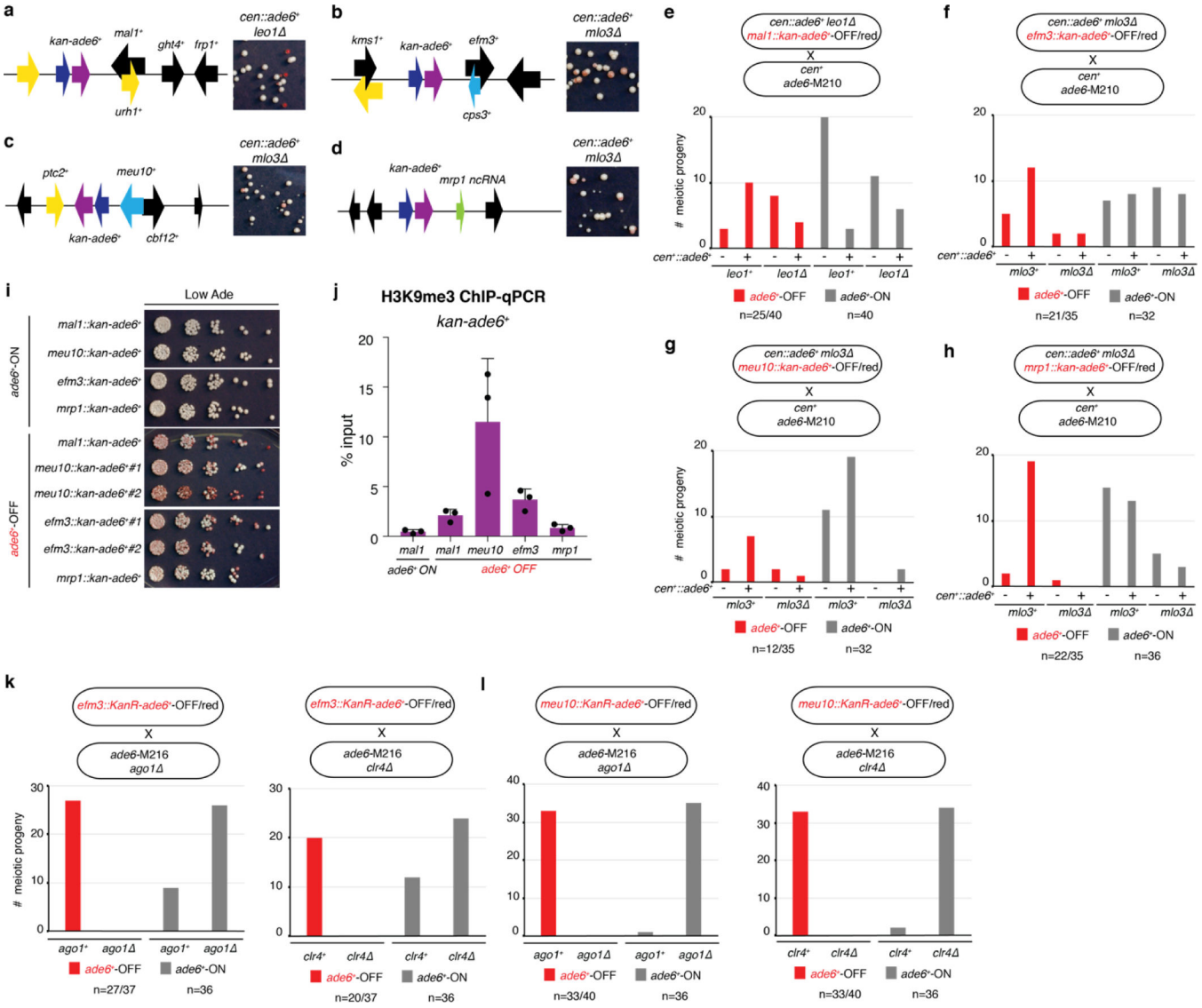

Extended Data Figure 7 |. Heritable silencing of a *KanR-ade6*$^{+}$ transgene inserted at 4 different genomic loci.

a-d, Schematic diagrams of *kan-ade6*$^{+}$ insertions at the *mal1*$^{+}$ (**a**), *efm3*$^{+}$ (**b**), *meu10*$^{+}$ (**c**), and *mrp1*$^{+}$ (**d**) loci. **e-h,** *KanR-ade6*$^{+}$-OFF cells of the indicated genotypes were crossed to *cen1*$^{+}$ *ade6-M210* cells followed by random spore analysis. The number of progeny matching each genotype and phenotype are shown. Total red or white colonies genotyped are indicated for each cross. For red cells, the first number indicates kanamycin-resistant colonies (indicating presence of the *KanR-ade6*$^{+}$*-OFF* transgene) and second number indicates total red colonies (the remainder of which possess the endogenous *ade6-M210* mutant allele). **i,** *cen*$^{+}$ *KanR-ade6*$^{+}$ *mlo3*$^{+}$ *leo*$^{+}$ progeny of the crosses in (**e**)-(**h**) were plated on media containing low adenine to test for stability of each epiallele during mitotic growth. Performed once. **j,** ChIP-qPCR assay showing enrichment of H3K9me3 at *KanR-ade6*$^{+}$ epialleles in the *cen*$^{+}$ *mlo3*$^{+}$ *leo1*$^{+}$ progeny of the crosses in (**e**)-(**h**). Sample mean +/− SD from 3 biological replicates. **k-l,** *efm3::KanR-ade6*$^{+}$-OFF (**k**) or *meu10::KanR-ade6*$^{+}$-OFF

(**l**) cells were crossed to *ade6-M216 ago1Δ* (left) or *clr4Δ* (right), followed by RSA. All *ade6*$^{+}$-OFF progeny were *ago1*$^{+}$ and *clr4*$^{+}$. Bars indicate the number of *ade6*$^{+}$-OFF meiotic progeny for each genotype. Total red or white colonies genotyped are indicated for each cross. For red cells, the first number indicates kanamycin-resistant colonies (reflecting the presence of the *KanR-ade6*$^{+}$*-OFF* transgene) and the second number indicates the total red colonies (the remainder of which possess only the *ade6-M210* allele).

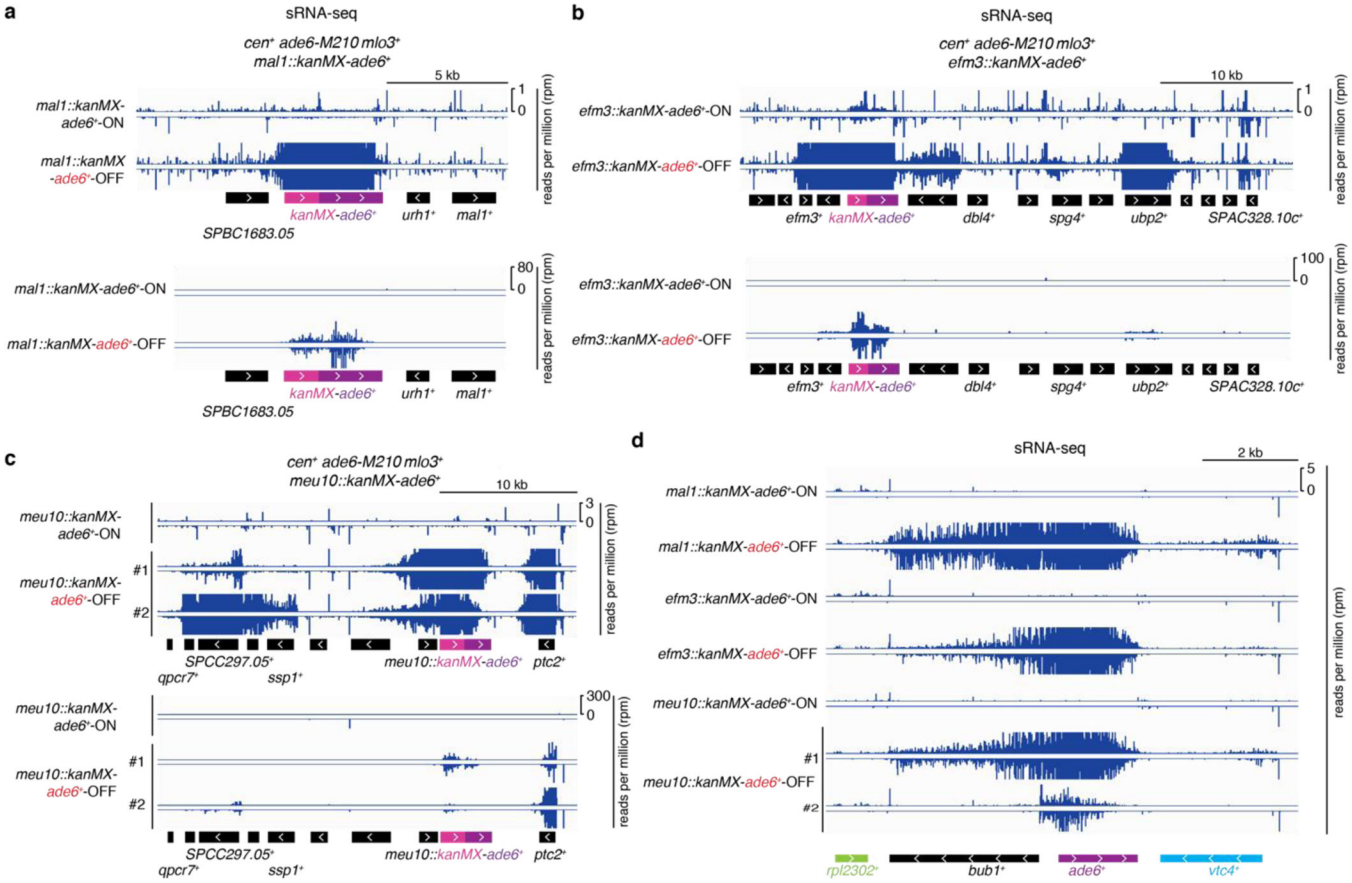

Extended Data Figure 8 |. Heritable silencing of *KanR-ade6*$^{+}$ transgenes correlates with local secondary siRNA generation.

a-c, Zoomed in (upper) or zoomed out (lower) sRNA-seq reads mapping to the indicated *KanR-ade6*$^{+}$ transgenes in *cen*$^{+}$ *mlo3*$^{+}$ *leo1*$^{+}$ meiotic progeny of the crosses in Extended Data Fig. 7e-g. In (**c**), two different red clones are shown, corresponding to clone #1 (upper) and clone #2 (lower) in Extended Data Fig. 7i. In these clones, the magnitude of locally hopped siRNAs (not mapping to *KanR-ade6*$^{+}$) correlates with the magnitude and efficiency of inherited silencing. **d,** Zoomed in view of sRNA-seq reads mapping to the endogenous *ade6*$^{+}$ locus. Sequencing was performed once, but for *ade6*$^{+}$-OFF *meu10::kanMX*, which represented a strong silent epiallele, small RNAs from 2 independent clones (#1 and #2) were analyzed.

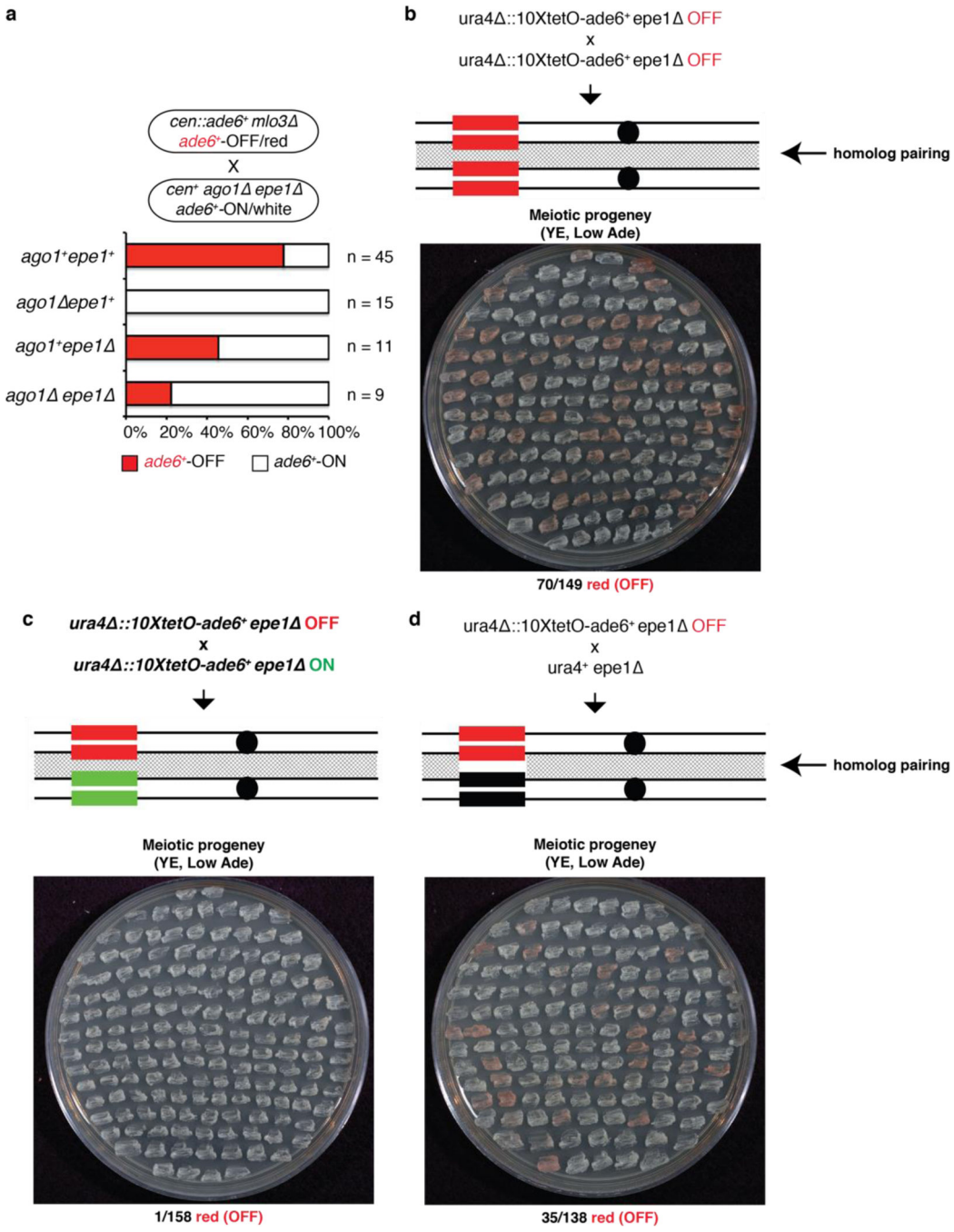

Extended Data Figure 9 |. Erasure of the silent state during diploid formation and meiosis requires interallelic pairing.

a, Biological replicate of the cross shown in Fig. 4a. *cen::ade6*$^{+}$ *mlo3Δ ade6*$^{+}$-OFF cells were crossed to *cen*$^{+}$ *ago1Δ epe1Δ ade6*$^{+}$-ON cells, followed by random spore analysis. Number and phenotype of *mlo3*$^{+}$ progeny with the indicated genotypes and phenotypes (red = OFF, white = ON) are shown. *mlo3Δ* progeny were excluded. n, number of meiotic progeny analyzed. **b,** Mating of a *ura4Δ::10XtetO-ade6*$^{+}$ *epe1Δ* OFF allele with an identical OFF allele, followed by diploid formation and sporulation (meiosis) produces progeny in

which the OFF state is maintained at a high frequency (47%). Repeated twice. **c,** Mating of the *ura4Δ::10XtetO-ade6*$^{+}$ *epe1Δ* OFF allele with a genetically identical ON allele results in erasure of the OFF state in nearly all of the resulting meiotic progeny. Repeated twice. **d,** Partial disruption of pairing by replacement of *ura4Δ::10XtetO-ade6*$^{+}$ with *ura4*$^{+}$ partially restores the epigenetic maintenance of the OFF state. Repeated once.

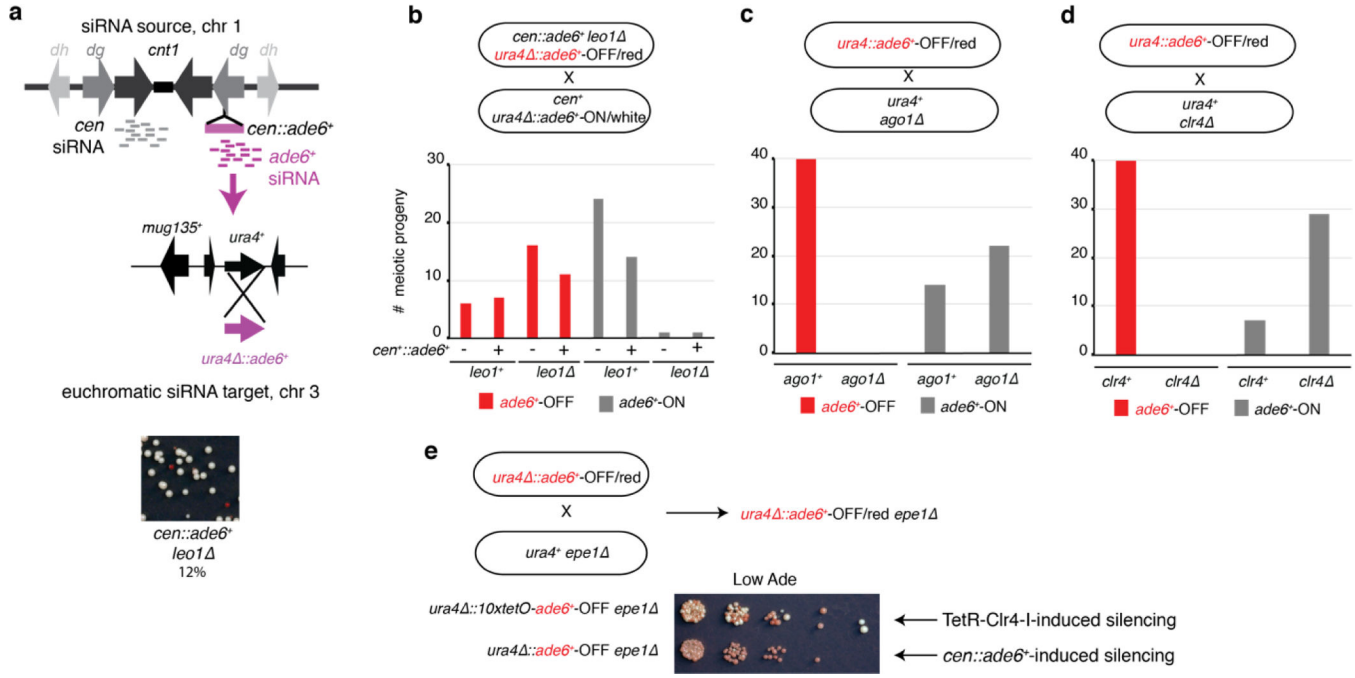

Extended Data Figure 10 |. Strategy for siRNA-induced silencing at the *ura4Δ::ade6*$^{+}$ locus.

a. The *ura4*$^{+}$ coding sequence was replaced with *ade6*$^{+}$ to generate a *ura4Δ::ade6*$^{+}$ allele in *cen::ade6*$^{+}$ *leo1Δ ade6-M210* cells. Formation of red colonies on low adenine medium indicated *ura4Δ::ade6*$^{+}$ silencing. **b,** *cen::ade6*$^{+}$ *leo1Δ ura4Δ::ade6*$^{+}$-OFF cells were crossed to *cen*$^{+}$ *ura4Δ::ade6*$^{+}$-ON cells to demonstrate that the resulting *ura4Δ::ade6*$^{+}$-OFF state is stable in the absence of the *cen::ade6*$^{+}$ siRNA trigger or the *leo1Δ* enabling mutation. **c, d.** Crosses showing that the *ura4Δ::ade6*$^{+}$-OFF epigenetic state depends on Ago1 (**c**) and Clr4 (**d**). **e,** Cross for generating an *epe1Δ ura4Δ::ade6*$^{+}$-OFF epiallele (top) and comparison of RNAi-independent (TetR-Clr4-I-induced) and RNAi-dependent (*cen::ade6*$^{+}$-induced) *ade6*$^{+}$-OFF epialleles. Same results were obtained with independent clones.

Supplementary Material

Refer to Web version on PubMed Central for supplementary material.

Acknowledgements

We thank members of the Moazed lab for helpful discussions, and Keith Connolly, Nahid Iglesias, Gloria Jih, and Gergana Shipkovenska for comments on the manuscript. R.Y. was partially supported by an NIH training grant (T32, GM96911). This work was supported by a grant from the NIH to D.M. (GM072805). D.M. is an investigator of the Howard Hughes Medical Institute.

References

1. Margueron R & Reinberg D Chromatin structure and the inheritance of epigenetic information. Nat Rev Genet 11, 285–296, doi:nrg2752 [pii] 10.1038/nrg2752 (2010). [PubMed: 20300089]
2. Moazed D Mechanisms for the inheritance of chromatin states. Cell 146, 510–518, doi:10.1016/j.cell.2011.07.013 (2011). [PubMed: 21854979]
3. Ragunathan K, Jih G & Moazed D Epigenetics. Epigenetic inheritance uncoupled from sequence-specific recruitment. Science 348, 1258699, doi:10.1126/science.1258699 (2015). [PubMed: 25831549]
4. Audergon PN et al. Epigenetics. Restricted epigenetic inheritance of H3K9 methylation. Science 348, 132–135, doi:10.1126/science.1260638 (2015). [PubMed: 25838386]
5. Wang X & Moazed D DNA sequence-dependent epigenetic inheritance of gene silencing and histone H3K9 methylation. Science 356, 88–91, doi:10.1126/science.aaj2114 (2017). [PubMed: 28302794]
6. Laprell F, Finkl K & Muller J Propagation of Polycomb-repressed chromatin requires sequence-specific recruitment to DNA. Science, doi:10.1126/science.aai8266 (2017).
7. Coleman RT & Struhl G Causal role for inheritance of H3K27me3 in maintaining the OFF state of a Drosophila HOX gene. Science, doi:10.1126/science.aai8236 (2017).
8. Verdel A et al. RNAi-mediated targeting of heterochromatin by the RITS complex. Science 303, 672–676, doi:10.1126/science.1093686,1093686[pii] (2004). [PubMed: 14704433]
9. Motamedi MR et al. Two RNAi complexes, RITS and RDRC, physically interact and localize to noncoding centromeric RNAs. Cell 119, 789–802, doi:S009286740401102X [pii] 10.1016/j.cell.2004.11.034 (2004). [PubMed: 15607976]
10. Volpe TA et al. Regulation of heterochromatic silencing and histone H3 lysine-9 methylation by RNAi. Science 297, 1833–1837 (2002). [PubMed: 12193640]
11. Sienski G et al. Silencio/CG9754 connects the Piwi-piRNA complex to the cellular heterochromatin machinery. Genes Dev 29, 2258–2271, doi:10.1101/gad.271908.115 (2015). [PubMed: 26494711]
12. Yu Y et al. Panoramix enforces piRNA-dependent cotranscriptional silencing. Science 350, 339–342, doi:10.1126/science.aab0700 (2015). [PubMed: 26472911]
13. Law JA & Jacobsen SE Establishing, maintaining and modifying DNA methylation patterns in plants and animals. Nat Rev Genet 11, 204–220, doi:10.1038/nrg2719 (2010). [PubMed: 20142834]
14. Luteijn MJ & Ketting RF PIWI-interacting RNAs: from generation to transgenerational epigenetics. Nat Rev Genet 14, 523–534, doi:10.1038/nrg3495 (2013). [PubMed: 23797853]
15. Iida T, Nakayama J & Moazed D siRNA-mediated heterochromatin establishment requires HP1 and is associated with antisense transcription. Mol Cell 31, 178–189, doi:S1097-2765(08)00464-4 [pii] 10.1016/j.molcel.2008.07.003 (2008). [PubMed: 18657501]
16. Yu R, Jih G, Iglesias N & Moazed D Determinants of heterochromatic siRNA biogenesis and function. Mol Cell 53, 262–276, doi:10.1016/j.molcel.2013.11.014 (2014). [PubMed: 24374313]
17. Kowalik KM et al. The Paf1 complex represses small-RNA-mediated epigenetic gene silencing. Nature 520, 248–252, doi:10.1038/nature14337 (2015). [PubMed: 25807481]
18. Allshire RC, Javerzat JP, Redhead NJ & Cranston G Position effect variegation at fission yeast centromeres. Cell 76, 157–169. (1994). [PubMed: 8287474]
19. Thakurta AG, Gopal G, Yoon JH, Kozak L & Dhar R Homolog of BRCA2-interacting Dss1p and Uap56p link Mlo3p and Rae1p for mRNA export in fission yeast. EMBO J 24, 2512–2523, doi:10.1038/sj.emboj.7600713 (2005). [PubMed: 15990877]
20. Jih G et al. Unique roles for histone H3K9me states in RNAi and heritable silencing of transcription. Nature 547, 463–467, doi:10.1038/nature23267 (2017). [PubMed: 28682306]
21. Grewal SI & Klar AJ Chromosomal inheritance of epigenetic states in fission yeast during mitosis and meiosis. Cell 86, 95–101 (1996). [PubMed: 8689692]

22. Gaydos LJ, Wang W & Strome S Gene repression. H3K27me and PRC2 transmit a memory of repression across generations and during development. Science 345, 1515–1518, doi:10.1126/science.1255023 (2014). [PubMed: 25237104]

23. Trewick SC, McLaughlin PJ & Allshire RC Methylation: lost in hydroxylation? EMBO Rep 6, 315–320, doi:10.1038/sj.embor.7400379 (2005). [PubMed: 15809658]

24. Ronshaugen M & Levine M Visualization of trans-homolog enhancer-promoter interactions at the Abd-B Hox locus in the Drosophila embryo. Dev Cell 7, 925–932, doi:10.1016/j.devcel.2004.11.001 (2004). [PubMed: 15572134]

25. Chen JL et al. Enhancer action in trans is permitted throughout the Drosophila genome. Proc Natl Acad Sci U S A 99, 3723–3728, doi:10.1073/pnas.062447999 (2002). [PubMed: 11904429]

26. Wong KH & Struhl K The Cyc8-Tup1 complex inhibits transcription primarily by masking the activation domain of the recruiting protein. Genes Dev 25, 2525–2539, doi:10.1101/gad.179275.111 (2011). [PubMed: 22156212]

27. Moreno S, Klar A & Nurse P Molecular genetic analysis of fission yeast Schizosaccharomyces pombe. Methods in enzymology 194, 795–823 (1991). [PubMed: 2005825]

28. Halic M & Moazed D Dicer-independent primal RNAs trigger RNAi and heterochromatin formation. Cell 140, 504–516, doi:S0092-8674(10)00020-6 [pii] 10.1016/j.cell.2010.01.019 (2010). [PubMed: 20178743]

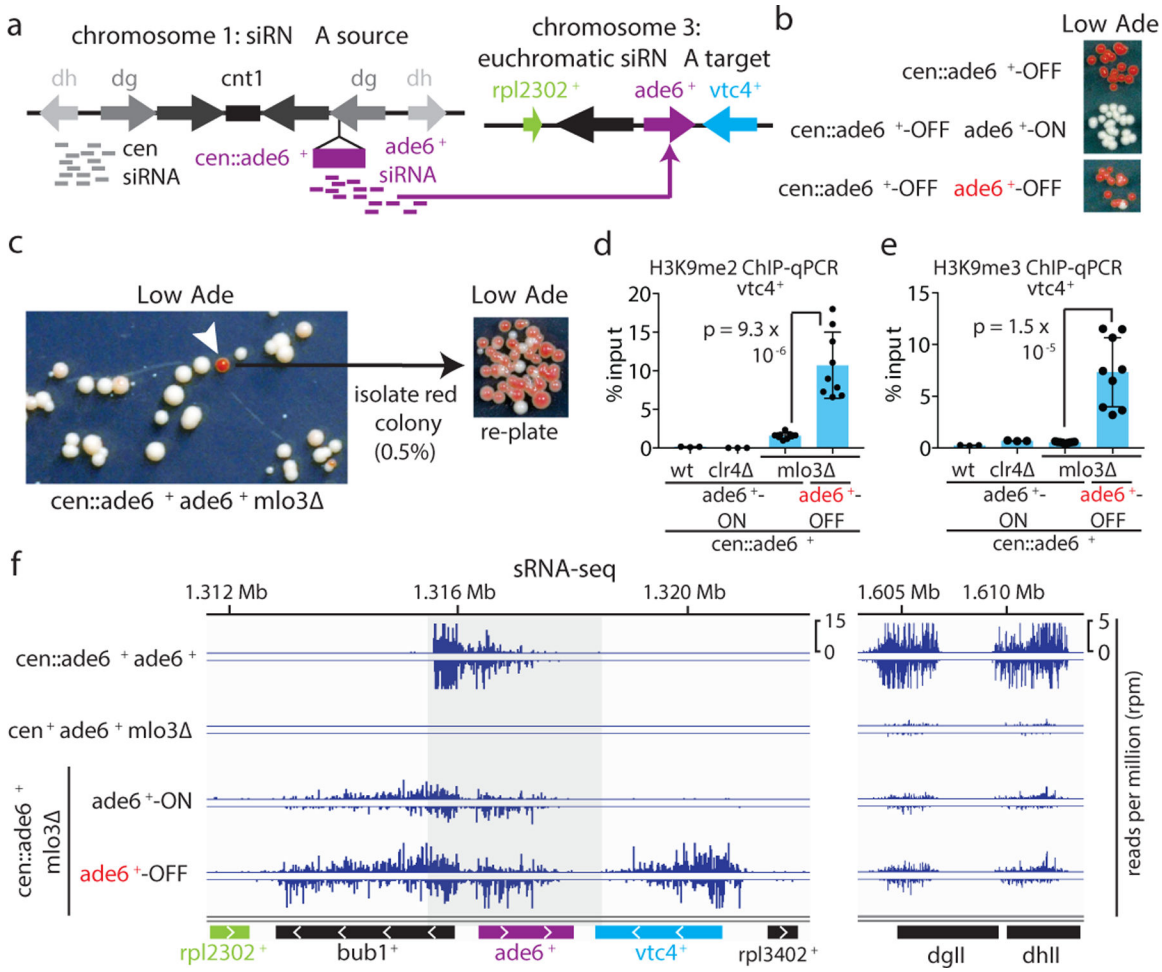

Figure 1 |. Establishment of siRNA-mediated silencing at the euchromatic *ade6*$^+$ locus is associated with local siRNA generation and H3K9 methylation

a, Schematic of the *cen::ade6*$^+$ siRNA driver (left) and euchromatic *ade6*$^+$ target (right) loci.

b, Expected phenotypes of cells containing the silenced *cen::ade6*$^+$ locus alone or in combination with the euchromatic *ade6*$^+$ in either expressed (ON/red) or silenced (OFF/red) states.

c, *cen::ade6*$^+$ *mlo3*Δ cells were plated on low adenine medium. ~0.5% of cells formed red or pink colonies, indicating silencing of euchromatic *ade6*$^+$ (white arrow). Repeated three times with similar results.

d-e, ChIP-qPCR assays showing H3K9me2 (**d**) or H3K9me3 (**e**) in *ade6*$^+$-OFF (red) compared to *ade6*$^+$-ON (white) cells at *vtc4*$^+$. Sample means +/− SD from 3 (*wt*, *clr4*Δ) or 9 (*mlo3*Δ) biological replicates (reflecting 3 independent clones); *p* values resulting from a 2-tailed Student's t-test.

f, Left, siRNA-sequencing showing increased secondary siRNA generation in *ade6*$^+$-OFF compared to *ade6*$^+$-ON cells. Note that for the *ade6*$^+$ gene itself and the immediately flanking sequences, the siRNA and H3K9me signals at the euchromatic and centromeric copies cannot be distinguished (shaded area represent sequence identity). Right, siRNAs mapping to the pericentromeric repeats (*dgII* and *dhII*) of chromosome 2 shown as controls.

Sequencing was performed once but see Fig. 3e, ED Fig. 3d, and ED Fig 8d for related results.

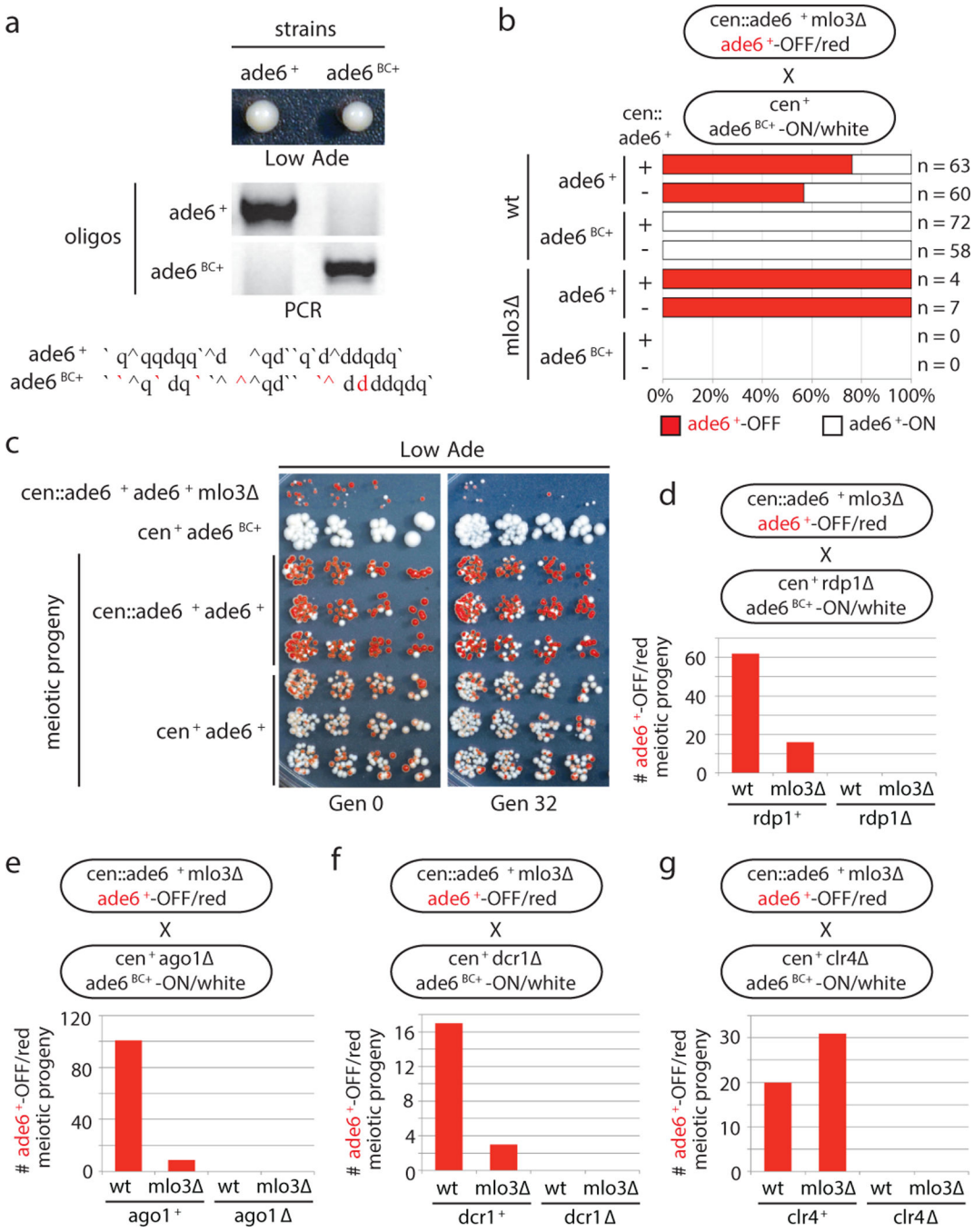

Figure 2 |. Maintenance of acquired silencing in wild-type cells and its dependence on RNAi and Clr4.

a, Top, the barcoded *ade6*$^{BC+}$ allele was functional as shown by formation of a white colony on Low Ade medium; *ade6*$^{+}$ served as a control. Bottom, sequences of the *ade6*$^{+}$ and *ade6*$^{BC+}$ alleles, base changes indicated in red. Allele-specific PCRs distinguish barcoded and wild-type alleles. Repeated >10 times with similar results.

b, *cen::ade6*$^{+}$ *ade6*$^{+}$-OFF *mlo3Δ* cells were crossed to *cen*$^{+}$ *ade6*$^{BC+}$-ON cells followed by random spore analysis (RSA). The frequency with which silencing in the progeny with the

indicated genotypes was maintained is shown. n, number of progeny analyzed. Repeated 3 times.

c, The progeny from the cross in panel b were grown for 0 or 32 generations and plated on Low Ade medium. Heritable silencing, as indicated by the growth of red/pink colonies, for both *cen*$^{+}$ and *cen::ade6*$^{+}$ progeny is apparent for 32 generations. Performed once, see ED Fig. 2a for related results.

d-g, *cen::ade6*$^{+}$ *mlo3Δ ade6*$^{+}$-OFF cells were crossed to *cen*$^{+}$ *mlo3*$^{+}$ *ade6*$^{BC+}$-ON cells with deletions of key RNAi components (**d-f**), or H3K9 methyltransferase *clr4*$^{+}$ (**g**), followed by RSA. All *ade6*$^{+}$-OFF progeny were *RNAi*$^{+}$ and *clr4*$^{+}$. Bars indicate number of *ade6*$^{+}$-OFF meiotic progeny for each genotype. Repeated in ED Fig. 2b-e with similar results.

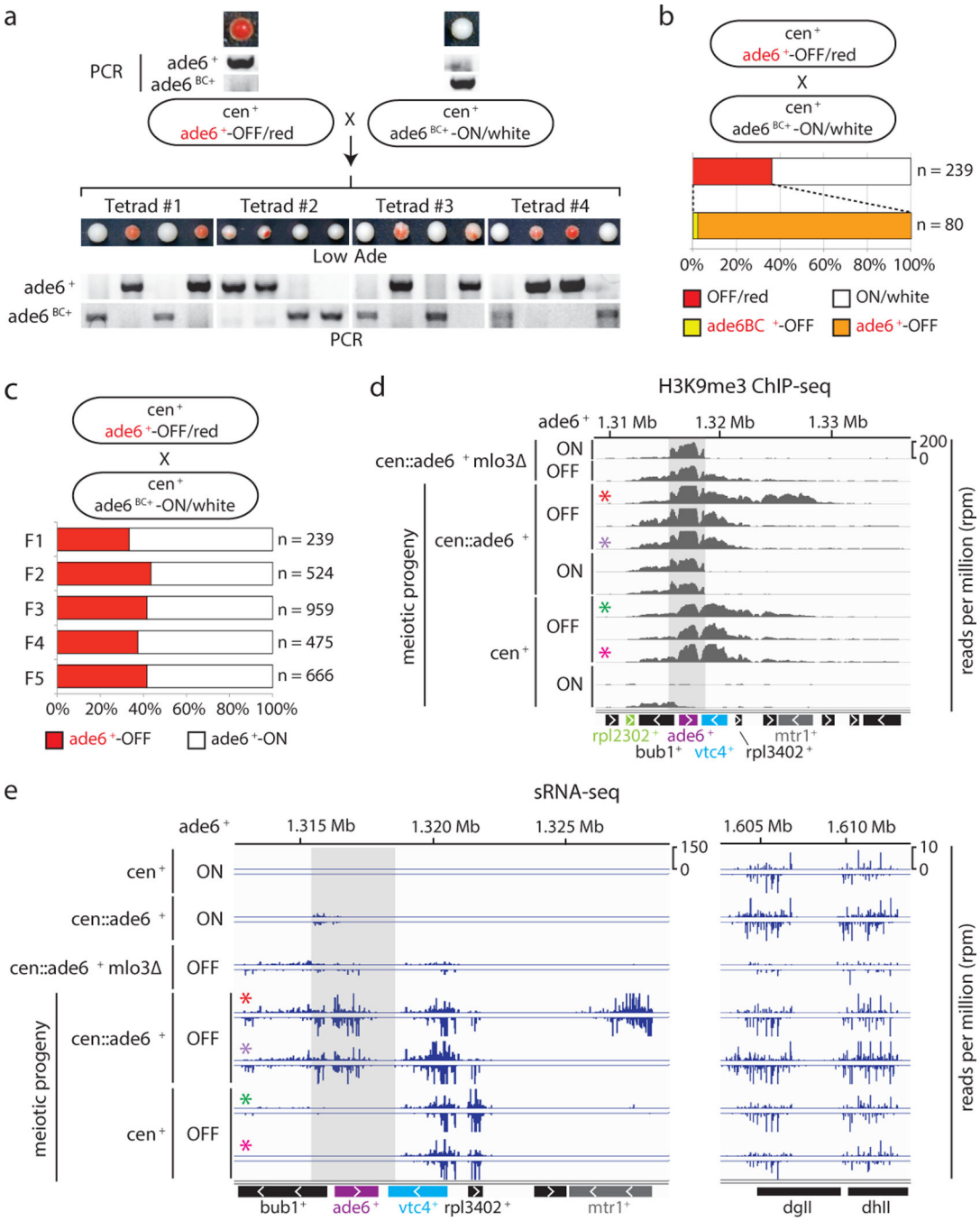

Figure 3 |. *Cis* inheritance of the silent *ade6*$^{+}$ epiallele and its association with H3K9me3 and secondary siRNA generation.

a, *ade6*$^{+}$-OFF cells crossed to *ade6*$^{BC+}$-ON cells, followed by tetrad dissection on Low Ade medium (top) and genotyping using allele-specific PCRs (bottom), showed the 2:2 segregation of the OFF and ON states and *cis* transmission of each state. See ED Fig. 4a for the reciprocal cross showing similar results.

b, *ade6*$^{+}$-OFF cells were crossed to *ade6*$^{BC+}$-ON cells, followed by random spore analysis. 80 out of 220 haploid meiotic progeny (36%) maintained silencing of *ade6*$^{+}$, largely in *cis* (78 out of 80 cells). Repeated 3 times with similar results.

c, *ade6*$^{+}$-OFF progeny of repeated *ade6*$^{+}$-OFF x *ade6*$^{BC+}$-ON crosses were selected and crossed again, showing stability of the *ade6*$^{+}$-OFF allele over five meiotic generations. n, number of meiotic progeny analyzed. Repeated with similar results in ED Fig 4b.

d, H3K9me3 ChIP-seq reads mapping to the euchromatic *ade6*$^{+}$ locus in cells with the indicated genotypes and expression states. Colored asterisks indicate ChIP- and sRNA-sequencing (shown in panel **e**) of the same clones. Shaded area, region of sequence identity with *cen::ade6*$^{+}$. 2–3 independent clones were analyzed for each ON and OFF meiotic progeny.

e, sRNA-seq reads mapping to the *ade6*$^{+}$ locus in cells with the indicated genotypes and expression states at the euchromatic *ade6*$^{+}$ locus (left) and the pericentromeric repeats of chromosome 2 (*dgII* and *dhII*) (right). Shaded area and colored asterisks as described in panel **d** legend. 2 independent clones were analyzed for each OFF progeny.

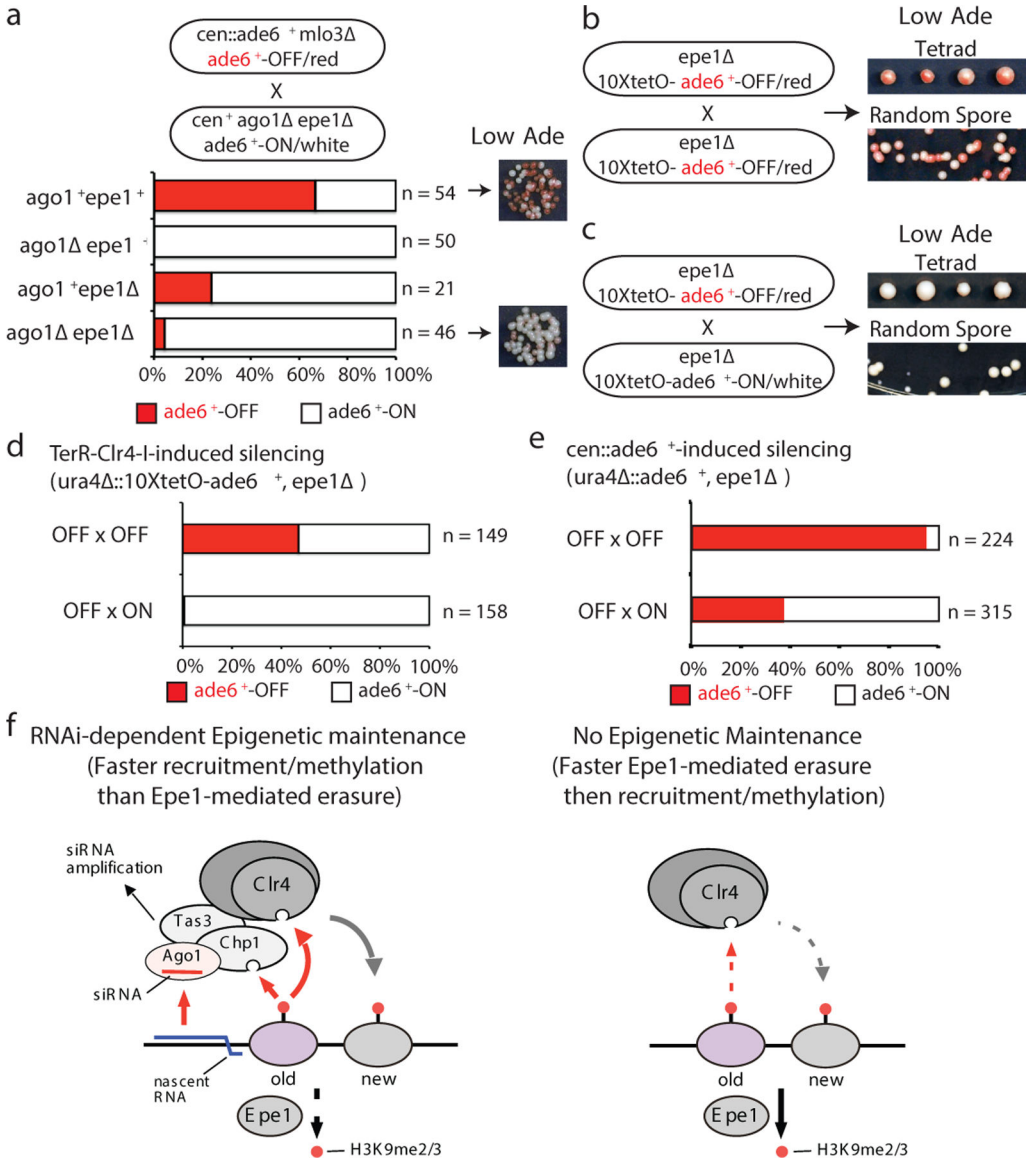

Figure 4 |. RNAi protects an acquired silent state against erasure by Epe1 or activation by an expressed homologous allele.

a, *cen::ade6*$^{+}$ *mlo3Δ ade6*$^{+}$-OFF cells were crossed to *cen*$^{+}$ *ago1Δ epe1Δ ade6*$^{+}$-ON cells, followed by random spore analysis. Number and phenotype of *mlo3*$^{+}$ progeny with the indicated genotypes and phenotypes are shown. *mlo3Δ* progeny were excluded. On the right, growth on Low Ade medium indicated meiotic progeny showing maintenance of the *ade6*$^{+}$-OFF state in *ago1Δ epe11Δ* cells. All *ago1Δ epe1*$^{+}$ progeny formed white colonies indicating loss of the silent state. n, number of meiotic progeny analyzed.

b-d, *epe1Δ ura4Δ::10xtetO-ade6*$^{+}$-OFF cells were crossed to either *epe1Δ ura4Δ::10xtetO-ade6*$^{+}$-OFF (**b**) or *epe1Δ ura4Δ::10xtetO-ade6*$^{+}$-ON (**c**) cells, followed by tetrad dissection (top) or random spore analysis (bottom). Quantification of ON and OFF states in the progeny is shown in **d**. Silencing was initiated by siRNA-independent TetR-Clr4-I. n, total progeny.

e, Mating of a *ura4Δ::ade6*$^{+}$-OFF *epe1Δ* allele with either an OFF or ON allele, followed by diploid formation and sporulation (meiosis), showing that when silencing is established in an siRNA-dependent manner (*cen::ade6*$^{+}$ *leo1Δ*), the OFF state is protected from pairing-induced erasure. n, total progeny.

f, Model for the role of RNAi in allele-specific epigenetic inheritance. Left, the siRNA-programmed RITS complex, containing Ago1, Tas3, and Chp1, serves as an epigenetic sensor that maintains allele-specific gene silencing. When both H3K9me and local complementary siRNAs are present, RITS associates with the target locus and recruits the Clr4 methyltransferase complex to methylate histone H3K9 on newly deposited nucleosomes. RITS also promotes local siRNA amplification. Right, in the absence of local RNAi, H3K9me cannot be epigenetically maintained in *epe1*$^{+}$ cells.